Enhancing Temperature Control of Electric Furnaces Using a Modified Pid Controller Design Strategy

A. Idir, A. Zemmit, H. Akroum, M. Nesri, S. Guedida, Laurent Canale

Enhancing Temperature Control of Electric Furnaces Using a Modified Pid Controller Design Strategy

A. Idir

abdelhakim.idir@univ-msila.dz

University Mohamed Boudiaf of M'sila

A. Zemmit

University Mohamed Boudiaf of M'sila

H. Akroum

Université M'Hamed Bougara

M. Nesri

Ecole Supérieur Ali Chabati

S. Guedida

Ecole Militaire Polytechnique, UER ELT

L. Canale

CNRS, UMR 5213 Toulouse

Research Article

Keywords: Harris Hawks Optimization, FrOPID Controller Design, Temperature Control, Electric Furnace, Transient and Frequency Stability Analysis

Posted Date: September 25th, 2024

DOI: https://doi.org/10.21203/rs.3.rs-4967918/v1

Additional Declarations: No competing interests reported.

ENHANCING TEMPERATURE CONTROL OF ELECTRIC FURNACES USING A MODIFIED PID CONTROLLER DESIGN STRATEGY

A. Idir [1,2], A. Zemmit [1], H. Akroum [3], M. Nesri [4], S. Guedida [5] and L. Canale [6]

[1] *Electrical Engineering Department, University Mohamed Boudiaf of M'sila, 28000 M'sila, Algeria*
[2] *Applied Automation Laboratory, F.H.C, University of Boumerdes, 35000 Boumerdes, Algeria*
[3] *Laboratoire d 'Automatique Appliquée, Université M'Hamed Bougara, Boumerdès, Algeria*
[4] *Ecole Supérieur Ali Chabati, Reghaia Algiers, Algeria*
[5] *Ecole Militaire Polytechnique, UER ELT, 16111 Algiers, Algeria*
[6] *CNRS, LAPLACE Laboratory, UMR 5213* Toulouse, France

Abstract– This paper presents the design and implementation of a modified Proportional-Integral-Derivative (PID) control strategy, named the Fractionalized PID (FrOPID), to enhance the transient and frequency responses, as well as the robustness of temperature control in electric furnaces. The FrOPID controller introduced in this study is being used for the first time to control electric furnace temperature. The FrOPID controller is an extension of the traditional PID controller, requiring the adjustment of four parameters compared to the three parameters of the traditional PID controller. The effectiveness of the proposed FrOPID approach was validated through extensive analysis of transient and frequency responses, as well as robustness analysis. The performance of the proposed HHO/FrOPID controller was then benchmarked against several other controllers, including the PID controller optimized by the original Harris Hawks Optimization (HHO) algorithm, and those tuned using advanced meta-heuristic algorithms such as the Harris Hawks Optimization-based PID (HHO/PID), Modified Electric Eel Foraging Optimization-based PID (MEEFO/PID), Electric Eel Foraging Optimization-based PID (EEFO/PID), and Whale Optimization Algorithm-based PID (WOA/PID). Simulation results demonstrate that the proposed HHO/FrOPID controller outperforms other existing controllers, offering superior and more robust performance in terms of percentage overshoot, settling time, rise time, and peak time.

Key words: Harris Hawks Optimization, FrOPID Controller Design, Temperature Control, Electric Furnace, Transient and Frequency Stability Analysis.

1. Introduction

Electric furnaces are widely used across various industries. They convert electrical energy into thermal energy for the purpose of heating. Temperature regulation is a critical parameter that requires precise control in industrial and engineering applications. If the temperature is not properly controlled, the physical properties of the processed materials may be altered or degraded. Therefore, it is essential to maximize the precision and speed of control to ensure optimal performance. Numerous control techniques have been developed to address this challenge.

Effective management of electric furnaces is critical, as it directly influences the quality, productivity, and energy efficiency of industrial processes. Precise temperature regulation is essential to achieve the desired material

properties, prevent heat-related degradation, and optimize energy consumption. Inaccurate temperature control can lead to compromised product quality, increased energy costs, and greater environmental impact. Therefore, there is a strong need for the continuous advancement of control techniques [2–4].

Various methods are employed for temperature control in electric furnaces across industries. These include proportional-integral-derivative (PID) control, proportional-integral-derivative accelerated (PIDA) controller [5], fractional-order PID controller [6], continuous sliding-mode control (CSMC) [7], predictive control [8], and internal model control (IMC) [9]. However, over 90% of the Industry relies on PID controllers due to their ease of use, straightforward operation, and versatility in a wide range of applications [10].

Due to the non-linear characteristics of electric furnace systems, tuning PID controllers can be a challenging task for researchers. Additionally, system parameters may vary over time. Therefore, employing intelligent and adaptive control strategies is a more suitable option for fine-tuning PID controllers. Various optimization methods are available, even for controllers with similar structures. These methods have been proposed for optimizing controller settings, such as those used in regulating the temperature control of electric furnaces, one such technique is the Nelder-Mead (NM) approach [11], fuzzy logic (FL) [12], extended non-minimal state space fractional order model predictive control (EnMSSFMPC) [13], neural network [14], enhanced version of whale optimization algorithm (EWOA) [15], a modified electric eel foraging optimizer [16], genetic algorithm (GA) [17], adaptive fuzzy-neural network (AFNN) controller [18], .

Although the PID controller is still widely used, it is essential to develop and implement more advanced control techniques to enhance the overall performance, sustainability, and cost-effectiveness of industrial processes dependent on electric furnaces. However, the PID controller may exhibit prolonged settling times in systems with significant inertia and time delays, making it insufficient to meet the growing demands for control performance.

This research introduces a modified PID controller, known as a fractionalized Order PID (FrOPID) controller [19-21], marking the first documented application of this controller in the field of temperature regulation in electric furnaces. The FrOPID controller offers a notable advantage by effectively mitigating the kick effect through the incorporation of fractional order into the integral gain [22,23]. This enhancement improves the flexibility of the electric furnace temperature-control system by optimizing its transient and frequency responses while minimizing the adverse effects of disturbances. In addition to the proportional (K_p), integral (K_i), and derivative (K_d), parameters that make up the integer order PID, the FrOPID controller also has one more parameter: an integrator fractional order (α). This FrOPID uses an additional fractional order filter to approximate integer order transfers in the feedback control loop by maintaining the same overall equivalent closed-loop transfer function but adding

fractional order integrators (α) to the classical PID feedback control loop. Thus, FrOPID has four parameters, which is one more than the traditional PID.

The main contributions of this work are as follows:

- The proposed harris hawks optimization based Fractionalized order PID (HHO/FrOPID) controller is being introduced for the first time, marking its initial documented application in the field of temperature regulation for electric furnaces.
- This study presents a comparative analysis of the proposed FrOPID controller for temperature control technique, which integrates HHO Algorithm, against other state-of-the-art algorithms from the literature.
- The results clearly demonstrate that the proposed HHO/FrOPID controller significantly outperforms existing methods, delivering superior accuracy in key performance metrics such as overshoot, rise time, and settling time. This advancement highlights the efficacy of the FrOPID controller in achieving enhanced control precision for temperature regulation.

The paper is organized as follows: Section 2 details the mathematical modeling of the temperature control system. Section 3 presents the integration of the HHO algorithm with the fractional-order PID controller. In Section 4, comprehensive computer simulations are conducted, showcasing the superiority of the proposed algorithm through rigorous comparisons with previous studies. The results and in-depth discussions are covered in Sections 4 and 5. Robustness analysis is studied in Section 6. Finally, conclusions are drawn in Section 7.

2. Mathematical Model of Temperature control system

The electric furnace comprises a furnace, controller, temperature gauge, power regulator, sensor, and heating coil. In this setup, the sensor detects the temperature and generates a voltage signal that serves as negative feedback to the input, representing the desired temperature setting. The controller adjusts the power supplied to the electric furnace based on the error voltage.

Figure 1 shows the setup where the controller regulates the temperature within the electric furnace. It consists of an electric furnace, a controller, a thermocouple, and a heater. The system's purpose is to regulate the temperature within the furnace.

In Figure 1, the variable r represents the input voltage, U is the output voltage from the controller, y is the output voltage from the thermocouple, and R is the armature resistance.

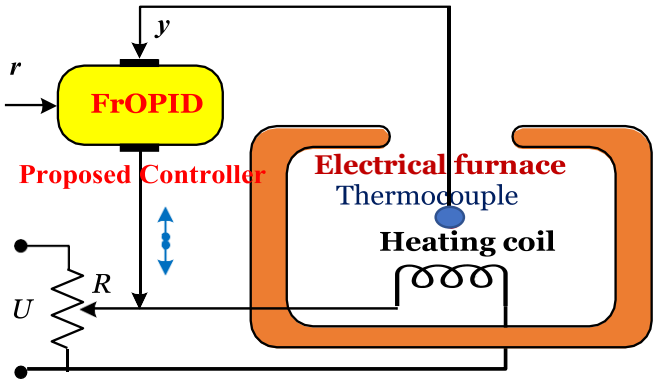

Figure 1. Block scheme of electric furnace control

The transfer function $G_p(s)$ of the electric furnace temperature system in the s-domain is expressed as a second-order system with time delay (SOSPD)**,** as shown in equation (1). The time delay, or transport lag, in equation (1) can be estimated using the first-order Padé approximation given in equation (2). Consequently, the transfer function of the electric furnace temperature system in equation (1) can be reformulated as shown in equation (3) [5,15,16,24].

$$G_p(s) = \frac{0.15}{s^2 + 1.1\,s + 0.2}\, e^{-1.5s} \tag{1}$$

$$e^{-1.5s} = \frac{1 - 0.75s}{1 + 0.75s} \tag{2}$$

$$G_p(s) = \frac{-0.1125s + 0.15}{0.75s^3 + 1.825s^2 + 1.25s + 0.2} \tag{3}$$

To better understand the system's behavior, we evaluate its step response without a controller, as shown in Figure 2.

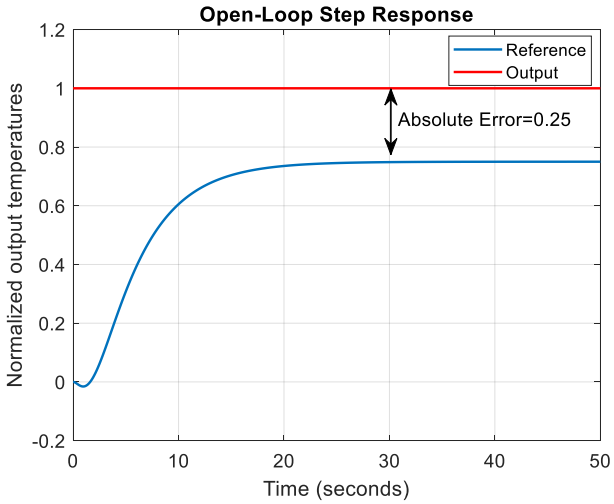

Figure 2. Step response of the system without the controller.

This reveals its inadequacy: the rise time and settling time are excessively long, and there is a significant offset error, defined as the difference between the reference input and the output. The reference step input is 1, while the output is approximately 0.75. Table 1 presents the measured values of settling time, rise time, and percentage overshoot for the uncontrolled system.

Table 1. Parameters measured without a controller

Parameters	Values
Rise time $[s]$	10.2
Settling time $[s]$	19.8
Overshoot [%]	0.00

3. Fractionalized Order PID Controller based on Harris Hawks optimization algorithm

3.1 Design fractionalized order PID (FrOPID) controller

This study analyzes the application of a fractionalized PID controller to the equation 3 transfer function of a feedback control for the electric furnace temperature control system.

Figure 3 shows an electric furnace temperature system under the FrOPID feedback control loop, with $G_p(s)$ and $G_c(s)$ representing plant and controller models. The controller manages output response $Y(s)$ based on input $R(s)$ and maintains response despite external disturbances $D(s)$.

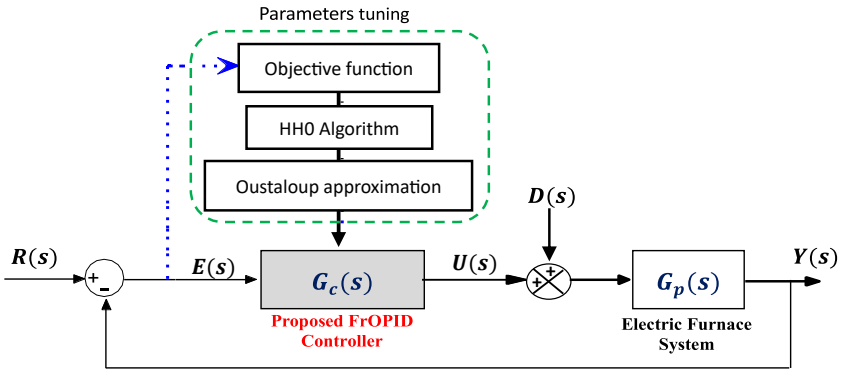

Figure 3. Proposed HHO based FrOPID Controller

The design of a traditional PID controller is represented by the following diagram:

$$G_c(s) = K_p\left(1 + \frac{1}{T_i s} + T_d s\right) \tag{4}$$

The enhancement of fractionalization in the control system element alters the PID control rule, resulting in the fractionalization of the integral operator $1/s$ [19,20,25]:

$$\frac{1}{s} = \frac{1}{s^{\alpha}} \cdot \frac{1}{s^{1-\alpha}} \tag{5}$$

The fractionalization of the classical PID controller to be developed is represented by [8,9]:

$$G_c(s) = K_p\left(1 + \frac{1}{T_i s} + T_d s\right) = \frac{1}{s}\left(\frac{K_p T_i T_d s^2 + K_p T_i s + K_p}{T_i}\right)$$
$$= \frac{1}{s^{\alpha} s^{1-\alpha}}\left(\frac{K_p T_d s^2 + K_p T_i s + K_p}{T_i}\right) \quad (6)$$

Where, $0 < \alpha < 1$.

In this study, integral absolute error (IAE) is chosen as the performance criterion for HHO. Calculation of the error $e(t)$ involves determining the difference between the reference model and the actual model. A smaller error value indicates closer approximation to the desired controller parameters.

$$J(K_p, K_i, K_d) = IAE = \int_0^{t_{sim}} |e(t)|dt \quad (7)$$

The letter J denotes the performance criteria, indicating the degree of resemblance between the controlled object and the reference model, while $e(t)$ represents the error signal. Here, $e(t)$ corresponds to the disparity between the reference speed and the actual speed $(v_{ref}(t) - v(t))$. The simulation time (t_{sim}) was set to 40 seconds for this investigation.

3.2 Harris Hawks optimization algorithm (HHOA)

The Harris Hawks optimization method is a population-based approach that mimics the hunting behavior of Harris' Hawks. It includes three main phases for its formulation [19,26].

- ***Exploration phase***

The algorithm involves Harris Hawks searching for prey at random locations using a wait-and-watch method. The Hawks' position is determined by $X(t+1)$, with $X_{rabbit}(t)$ and $X(t)$ being random numbers. The average position is calculated using $X_m(t)$, where the mean and total population are the same.

$$X(t+1) = \begin{cases} X_{\text{rand}}(t) - r_1|X_{\text{rand}}(t) - 2r_2X(t)| q \geq 0.5 \\ X_{\text{rab}}(t) - X_m(t) - r_3\big(L_b + r_4(U_b - L_b)\big) q < 0.5 \end{cases} \quad (8)$$

$$X_m(t) = \frac{1}{N}\sum_{i=1}^{N} X_i(t) \quad (9)$$

Where (r_1, r_2, r_3, r_4) are random numbers between $(0,1)$, (L_b, U_b) are the lower and upper bounds of variables, $X_{\text{rand}}(t)$ is a randomly selected hawk from the current position and N is the Hawks' total population.

- ***Exploration to exploitation transition***

The stage mimics the maneuvering techniques of Harris Hawks, which depend on the energy levels of their prey as it tries to escape. This effectively illustrates the energy dynamics of rabbits in such scenarios.

$$E = 2E_0\left(1 - \frac{t}{T_{\max}}\right) \tag{10}$$

The variables E,E_0 and $T_{\max}$ denote the energy of the escaping prey, the beginning energy of the prey, and the maximum number of iterations taken, respectively.

- ***Exploitation phase***

The final stage of the HHO algorithm involves four techniques based on the prey's energy level and escape potential. When $r > 0.5$ and $E > 0.5$, a soft besiege is executed, while for $r > 0.5$ and $E < 0.5$, a hard besiege is performed. When $r < 0.5$ and $E > 0.5$, a soft besiege with progressive rapid drive is carried out.

3.3 Oustaloup Approximation Method

The Oustaloup approximation approach is used to estimate the fractional-order (FO) integrator and differentiator [27,28]. Providing a precise representation of a fractional operator is the main goal of Oustaloup's approximation [28].

$$G(s) = S^{\alpha} \qquad ,(\alpha \in R) \tag{11}$$

Filter of Oustaloup is given by:

$$G(s) = K\prod_{k=1}^{N}\frac{s + \omega_k^{'}}{s + \omega_k} \tag{12}$$

The values of the zeros, poles, and gain are determined by:

$$\omega_k = \omega_b.\omega_u^{(2k-1+\gamma)/N}, \omega_k^{'} = \omega_b.\omega_u^{(2k-1-\gamma)/N}, K = \omega_h^{\gamma} \tag{13}$$

For $k = 1,2,\ldots,N$ with, $\omega_u = \sqrt{\omega_h/\omega_b}$

Where, ω_b is the lower bound, ω_h is the upper bound, γ is the derivative order and N is the order of filter.

3.4 Reduced order approximation

The Oustaloup method produces integer models of very high order to achieve the desired precision. However, implementing and simulating these higher-order models can be quite challenging. To address this, it is necessary to reduce the model's complexity, either by simplifying it or by using a lower-order model, while preserving the essential features and characteristics of the original integer-order model.

Figure 4 illustrates the error signal for model reduction, alongside the original model.

$$G(s) = \frac{b_1 s^{n-1} + \cdots + b_{n-1}s + b_0}{s^n + a_1 s^{n-1} + \cdots + \alpha_{n-1}s + a_n} \tag{14}$$

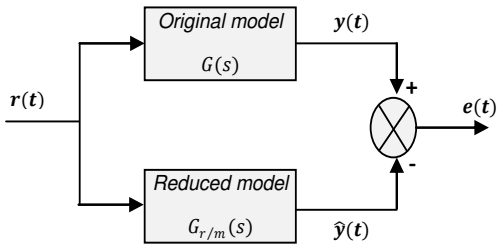

Figure 4. Error signal for model reduction

As noted in references [19,29], our current goal is to find a low-order approximation of an integer-order model.

$$G_{r/m}(s) = \frac{\beta_1 s^{\mathrm{r}} + \cdots + \beta_r s + \beta_{r+1}}{s^{\mathrm{m}} + \alpha_1 s^{m-1} + \cdots + \alpha_{m-1} s + \alpha_m} \tag{15}$$

The Laplace transform of the error signal can be expressed as:

$$E(s) = G(s) - G_{r/m}(s) \tag{16}$$

Where $R(s)$represents the Laplace transform of the input signal $r(t)$.

The objective function for minimizing the H_2 −norm of the reduction error signal is given by:

$$J = \min_{\theta} \left\| \hat{G}(s) - G_{r/m}(s) \right\|_2 \tag{17}$$

Where θ represents the parameters that are adjusted to ensure that:

$$\theta = [\beta_1, \ldots, \beta_r, \alpha_1, \ldots, \alpha_m] \tag{18}$$

Where J is the performance criterion and $G_{r/m}(s)$ is the reduced-order model.

4. Results and Discussion

The optimal gains for a PID controller were determined using the Harris Hawks Optimization (HHO) algorithm, with a MATLAB/Simulink model for an electric furnace temperature control system. The gains for the PID controller were represented as a vector of real values corresponding to each Harris Hawk in the population. The HHO algorithm was employed to design the PID controller for the system model $G_p(s)$,, and the closed-loop transfer function was subsequently derived.

The following provides the transfer function of a FrOPID controller, where the proportional, integral, and derivative gains are represented by K_p, K_i, and K_d and fractional integral order α, respectively. Table 2 lists the parameters of the proposed HHO algorithm. This algorithm was employed to design a PID controller for the system model $G_p(s)$ as shown in Eq. 3, with the PID parameters set to $K_p = 3.2920$, $K_i = 0.6205$, and $K_d = 4.3618$.. The

closed-loop transfer function of the temperature control system, which incorporates the fractional PID controller and unity feedback, is given by:

$$G_{CL\_FrOPID}(s) = \frac{G_{HHO-FroPID}(s)^{*}G_p(s)}{1 + G_{HHO-FrOPID}(s) * G_p(s)} \tag{19}$$

Table 2. HHOA-PID parameters for solving optimization problem

Hawks Number (population size)	50
Maximum iteration number	40
levy flight function constant	1.5
Lower bound for $[K_p,\ K_i, K_d]$	[0.01;0.01;0.01]
Upper bound for $[K_p,\ K_i, K_d]$	[5;5;5]
Optimization problem dimension	3
Simulation time	40s

The closed-loop transfer function is "fractionalized" in Equation (20), with the integrator's fractional order $\alpha = 0.5$ approximated using the Oustaloup technique. The approximation parameters are $\omega_b = 0.1\ rad/s,\ \omega_h = 10\ rad/s$. The HHO algorithm employs unity feedback.

$$G_{HAO/HHO-FrOPID}(s) = \frac{\begin{array}{c}-0.04907s^{13} - 1.254s^{12} - 12.29s^{11} - 58.6s^{10} - 141.8s^{9} - \\ 144.9s^{8} + 57.48s^{7} + 317.5s^{6} + 369.1s^{5} + 225.9s^{4} + \\ 81.22s^{3} + 17.15s^{2} + 1.959s + 0.09308\end{array}}{\begin{array}{c}0.7009s^{13} + 12.94s^{12} + 98.6s^{11} + 414.1s^{10} + \\ 1088s^{9} + 1924s^{8} + 2374s^{7} + 2066s^{6} + 1258s^{5} + \\ 526.2s^{4} + 146.8s^{3} + 25.92s^{2} + 2.606s + 0.1131\end{array}} \tag{20}$$

In order to demonstrate the efficiency and superiority of the suggested HHO/FrOPID method, we conduct a comparison between the HHO/FrOPID controller and both the original HHO/PID [16,26] controller and several other approaches found in existing literature. All of these approaches utilize the same parameters for electric heating furnaces, namely modified electric eel foraging optimization based PID (MEEFO/PID) [16], electric eel foraging optimization (EEFO/PID) [30], and Whale optimization algorithm based PID (WOA/PID) [16,31]. These strategies have shown to provide the most advantageous controller parameters up to this point. Readers may readily verify the results of this study using MATLAB commands such as "step," "stepinfo," "bode," "margin," and "bandwidth." Additionally, we emphasize the most outstanding outcomes from the comparison study by using bold formatting. The noteworthy discoveries of this investigation are further explained in the following subsections.

4.1 Transient Response Analysis

The selection of a suitable objective function also impacts the possibility of obtaining enhanced system performance. This function is crucial for maximizing both the system's dynamic reactivity and stability. The IAE

criterion was used as the goal function in this work to attain optimal system performance, as described in equation (7).

Table 3 presents the PID controller settings that correspond to the lowest value of the IAE objective function for different controllers selected for a fair comparison.

Table 3. The proposed controller's gain parameters and other controllers compared.

Controllers	K_p	K_i	K_d	N	α
HHO/FrOPID [Proposed]	3.2920	0.6205	4.3618	-	0.5
MEEFO/PID	3.2995	0.6156	4.4621	368.4193	-
EEFO/PID	3.1365	0.5925	4.1063	482.4784	-
WOA/PID	3.3376	0.5802	4.0353	86.5032	-
HHO/PID	3.2920	0.6205	4.3618	247.8975	-

The closed-loop system utilizing the Proportional-Integral-Derivative (PID) control scheme based on the Harris Hawks Optimization (HHO) algorithm exhibits a high level of complexity (order 13th; see equation. 20). Consequently, the overall memory capacity of the fractionalized PID controller will be decreased to better fit within the corrective loop (see subsection 3.4).

Equation (21) shows the low-order closed-loop transfer function corresponding to the high-order closed-loop system outlined in Equation (20). In this equation, the PID controller has been "fractionalized" using an integrator fractional order derived from the Oustaloup technique. The transfer functions of the HHO/PID, MEEFO/PID, EEFO/PID, and WOA/PID controllers are expressed in equations (22-25), utilizing the parameters listed in Table 3. These transfer functions are employed in the analyses carried out in the following subsections.

$$G_{HHO-FrOPID}(s) = \frac{-5.98s^3 + 5.209s^2 + 6.783s + 1.142 \times 10^{-9}}{s^5 + 9.683s^4 + 21.17s^3 + 23.22s^2 + 8.24s + 1.388 \times 10^{-9}} \tag{21}$$

$$G_{HHO-PID}(s) = \frac{122s^3 + 70.81s^2 + 105.2s + 23.07}{0.75s^5 + 187.7s^4 + 331.6s^3 + 380.9s^2 + 154.8s + 23.07} \tag{22}$$

$$G_{MEEFO-PID}(s) = \frac{-185.3s^3 + 110.3s^2 + 156.9s + 34.02}{0.75s^5 + 278.1s^4 + 488.3s^3 + 571s^2 + 230.6s + 34.02} \tag{23}$$

$$G_{EEFO-PID}(s) = \frac{-223.2s^3 + 127.3s^2 + 194.9s + 42.88}{0.75s^5 + 363.7s^4 + 658.5s^3 + 730.6s^2 + 291.4s + 42.88} \tag{24}$$

$$G_{WOA-PID}(s) = \frac{-39.65s^3 + 20.32s^2 + 37.75s + 7.528}{0.75s^5 + 66.7s^4 + 119.5\,s^3 + 128.8\,s^2 + 55.05s + 7.528} \tag{25}$$

Figure 5 shows the input-tracking responses of the electric furnace temperature control system, which utilizes a FrOPID controller developed by the HHO, as well as other controllers optimized by recent state-of-the-art techniques. Furthermore, Figure 6 provides a more detailed analysis of the step responses shown in Figure 5,

specifically focusing on key performance metrics such as overshoot (OS), rise time (T_r), settling time (T_s) and peak time (T_p) .

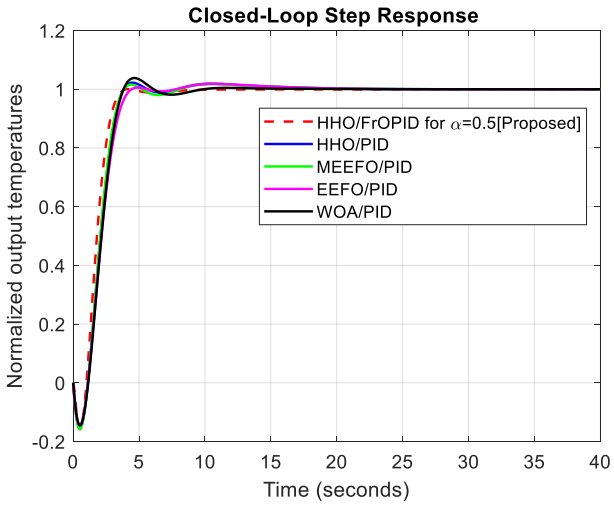

Figure 5. Performance Comparison of Input Tracking for Electric Furnace Temperature Control with Different Controllers

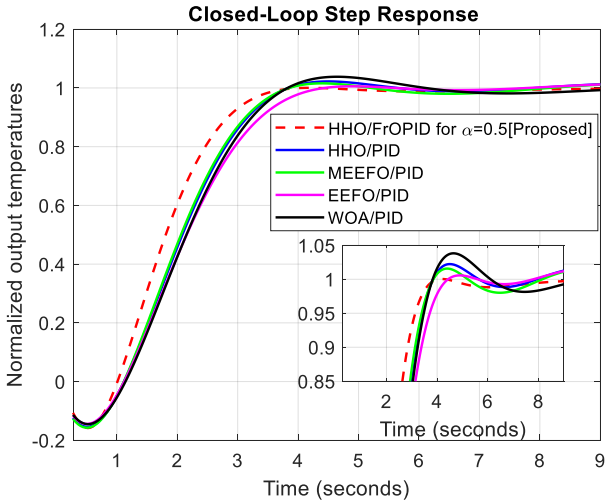

Figure 6. Zoomed-in view of Input-Tracking Performance Responses

Table 4 presents an analysis of the time-domain performance, including measures such as the maximum overshoot, rising time (measured from 10% to 90%), settling time (within a tolerance of ±2%), and peak time.

Table 4. Comparative Analysis of the Transient Response

Controllers	**Rise time (T_r) [s]**	**Settling time (T_s) [s]**	**Overshoot (OS)[%]**	**Peak time(T_p) [s]**
HHO/FrOPID [Proposed]	**1.6547**	**3.4335**	**0.1127**	**4.1842**
MEEFO/PID	1.8337	4.7686	2.2140	4.4270
EEFO/PID	1.8127	3.6223	1.7555	10.5467
WOA/PID	2.0340	4.0257	1.8420	10.7431
HHO/PID	1.8711	5.4817	3.8198	4.6407

Bold refers to the best-obtained value

The proposed HHO/FrOPID controller outperforms the others, demonstrating the fastest and most stable response, with the least overshoot and shortest peak time. The HHO/PID and MEEFO/PID controllers also offer good performance but are slightly less stable and slower in comparison. The EEFO/PID controller shows moderate performance, while the WOA/PID controller exhibits the least stability and the slowest response, making it the least effective option among the controllers analyzed.

4.2 Frequency Response Analysis

Figure 7 consists of two subplots, representing Bode plots typically used in control system analysis. Bode plots illustrate the frequency response of a system. The proposed FrOPID controller with $\alpha = 0.5$, optimized using the HHO, demonstrates potentially superior performance in specific frequency ranges. The magnitude plot suggests better control capabilities, while the phase plot indicates that the proposed method may offer faster response times and improved stability in comparison to traditional PID controllers optimized.

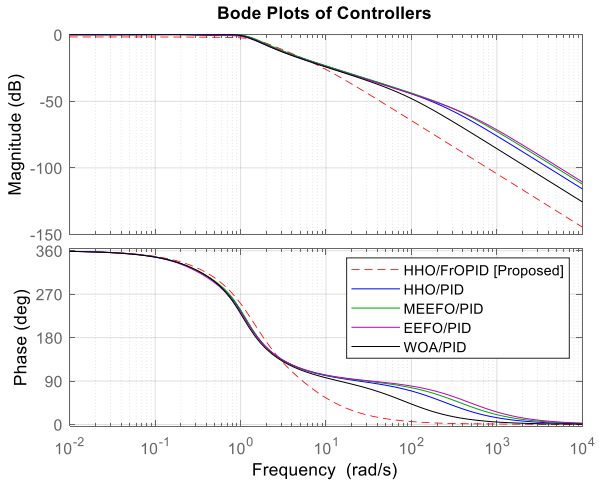

Figure. 7 Bode plots Comparison for different controller designs.

Table 5 presents the frequency stability metrics (gain and phase margin) and bandwidth for different controllers. The Gain Margin, a measure of gain robustness, indicates how much gain can be increased before instability. A higher gain margin indicates better stability. A higher phase margin indicates stability, while a higher bandwidth indicates faster response to input changes.

Table 5. Frequency Stability Metrics and Bandwidth

Controllers	Gain Margin (dB)	Phase Margin (deg)	Bandwidth (Hz)
HHO/FrOPID	**5.7045**	**Inf**	**1.6467**
HHO/PID	4.2858	140.84	1.4181
MEEFO/PID	4.1319	145.62	1.4525
EEFO/PID	5.0833	142.8	1.3027
WOA/PID	4.4898	70.957	1.3379

Bold refers to the best-obtained value

The HHO/FrOPID controller is distinguished by its exceptional gain margin, infinite phase margin, and greatest bandwidth, making it the top performer in terms of robustness, stability, and response speed. The EEFO/PID controller also performs well, with the second-highest gain margin and a substantial phase margin. Both the MEEFO/PID and HHO/PID controllers exhibit excellent stability and resilience, with the MEEFO/PID controller having a slight advantage in phase margin and bandwidth. In contrast, the WOA/PID controller has the smallest phase margin and modest bandwidth, indicating it is less reliable and somewhat slower in response compared to the other controllers. In summary, the HHO/FrOPID controller performs exceptionally well in all key areas, making it the most reliable and adaptable option among the controllers tested.

4.3 Performance evaluation via quality indicator

In this section, various error criteria and the Zwee-Lee-Gaing (ZLG) Quality Indicator are examined to assess the performance of the controllers.

4.3.1 Comparison of Different Error Criteria

When designing a PID controller, a crucial factor to consider is the error or discrepancy between the system's output and the desired target value. Using this error criterion as the fitness function during the optimization process often results in reduced overshoot but can lead to longer settling times. Fitness functions are typically based on error equations. The four standard error equations commonly used for this purpose, include Integral Time Absolute Error (ITAE), Integral Time Squared Error (ITSE), Integral Absolute Error (IAE), and Integral Squared Error (ISE).

$$ISE = \int e(t)^2 \cdot dt \tag{26}$$

$$IAE = \int |e(t)| \cdot dt \tag{27}$$

$$ITAE = \int t \cdot |e(t)| dt \tag{28}$$

$$ITSE = \int t \cdot [e(t)^2] \cdot dt \tag{29}$$

Where $e(t)$ is the error signal, defined as the difference between the desired output and the actual output.

Table 6 presents the performance of various controllers based on four different error criteria: IAE, ISE, ITAE, and ITSE. These indices are used as fitness functions to evaluate and compare the controllers' performance.

Table 6. Comparison of Performance Indices: ITAE, ITSE, IAE, and ISE as Fitness Functions.

Controllers	IAE	ISE	ITAE	ITSE
HHO/FrOPID	**2.0971**	**1.7931**	**2.9016**	**1.6811**
HHO/PID	2.4742	2.0501	4.5547	2.6876
MEEFO/PID	2.4589	2.0376	4.5506	2.6149
EEFO/PID	2.5435	2.0866	4.7739	2.9698
WOA/PID	2.4827	2.0915	3.7916	2.7426

Bold refers to the best-obtained value

As shown in Table 6, the HHO/FrOPID controller exhibits the best performance in terms of ITSE, with the lowest value of 1.6811, which indicates its effectiveness in minimizing time-weighted squared errors. It also performs well across other criteria, particularly in ISE, where it holds the second-lowest value, reflecting its overall robust performance. The bold values in the table highlight the best results for each error criterion. The HHO/FrOPID controller consistently achieves the most favorable outcomes, especially excelling in ITSE. This underscores its superior capability in minimizing time-weighted squared errors compared to other controllers. This comprehensive performance across various criteria demonstrates its robustness and effectiveness in optimizing control systems.

4.3.2 Comparison of Zwee-Lee-Gaing (ZLG) Quality Indicator

The ZLG indicator is a quantitative measure used to evaluate control system efficiency, combining transient response elements such as overshoot, settling time, rise time, and steady-state error. It is commonly used to compare control strategies and assess the dynamic response characteristics of a system under various controllers. Three approaches are available and are studied in this section: foundational quality assessment, comprehensive quality enhancement, and strategic quality innovation.

- Foundational Quality Assessment focuses on ensuring minimum standards for control system performance.
- Comprehensive Quality Enhancement builds on this by analyzing advanced performance metrics and continuous improvement indicators.
- Strategic Quality Innovation emphasizes innovative strategies to achieve superior control system performance, leveraging new technologies or methodologies.

The ZLG Quality Indicator is calculated as follows ($\boldsymbol{\delta} = 0.3679$):

$$ZLG = (1 - \delta)\left(OS + \left|T_{s\_min}\right|\right) + \delta(T_s - T_r) \tag{30}$$

Where:

- OS (Overshoot) is the maximum peak value of the response curve as a percentage of the input.
- T_{s_min} is the minimum value of the settling time range.
- T_s (SettlingTime) is the time required for the system's response to remain within a certain percentage (typically $2\%\ or\ 5\%$) of the final value.
- T_r (RiseTime) is the time required for the system's response to rise from a specified low percentage (typically 10%) to a specified high percentage (typically 90%) of the final value.
- δ (delta) is a weighting factor that balances the contribution of the different terms in the quality indicator.

The ZLG Quality Indicator is a quantitative measure used to assess control system performance, offering a numerical value for comparison. Table 7 presents the comparative values of the ZLG Quality Indicator for different

controllers evaluated using three distinct ZLG calculation approaches. These values illustrate how each controller performs under varying methodologies, highlighting their relative effectiveness.

Table 7. Comparative Values of ZLG Quality Indicator

Controllers	ZLG_Approach1	ZLG_Approach2	ZLG_Approach3
HHO/FrOPID	**1.1248**	**1.2373**	**1.0123**
HHO/PID	1.669	1.8359	1.5021
MEEFO/PID	1.2567	1.3824	1.131
EEFO/PID	1.314	1.4454	1.1826
WOA/PID	1.9392	2.1331	1.7453

Bold refers to the best-obtained value

As shown in Table 7, the proposed HHO/FrOPID controller exhibits the lowest ZLG Quality Indicator values among the evaluated controllers, particularly under ZLG_Approach3, where it achieves a value of 1.0123. This indicates the best performance for this approach. The HHO/FrOPID controller also performs relatively well across all approaches, suggesting its effectiveness in optimizing performance across different ZLG calculation methods. The bold values in the table highlight the best results for each approach, further demonstrating that the HHO/FrOPID controller consistently achieves the most favorable performance. This underscores its superior capability in optimizing control system performance compared to the other controllers.

5- Robustness analysis

Three scenarios are studied in this section:

Scenario 1: Response to a Step Change in Desired Temperature.

In this scenario, a step change in the desired temperature is tested. At $t = 30$ seconds, a step change of 0.5 is applied, and the results are displayed in Figure 8.

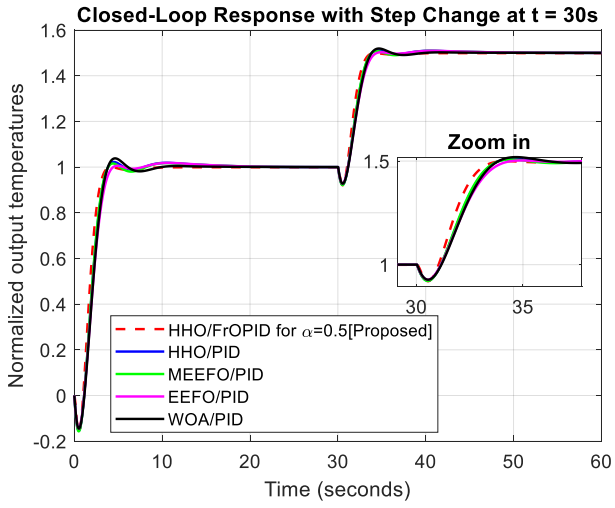

Figure 8. System Dynamic Performance in Scenario 1

The responses shown in this figure confirm the observations made in the subsection 4.1, indicating that the different controllers are effective in handling the step change in system input. However, the system with the proposed HHO/FrOPID controller demonstrates superior dynamic performance compared to the other controllers.

Scenario 2: Step Load Disturbance

This scenario involves examining the impact of a sudden change in load. The system experienced a step load disturbance, as illustrated in Figure 9. The corresponding dynamic responses are depicted in Figure 10. From these results, it is evident that using the proposed controller yields favorable settling time and overshoot.

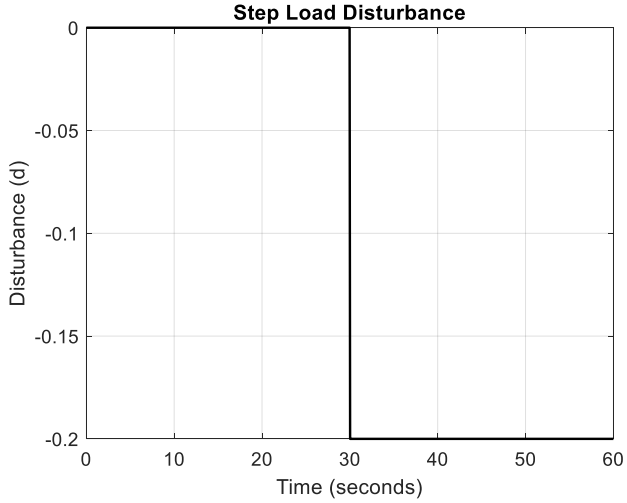

Figure 9. Step disturbance.

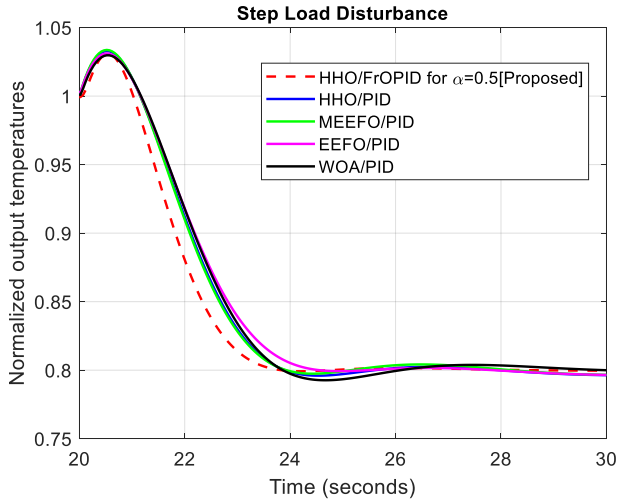

Figure 10. System Dynamic Performance of Scenario 2.

Scenario 3: A Random Reference Temperature

In this scenario, a random reference temperature was introduced to the system, as depicted in Figure 11, with the dynamic performance illustrated in Figure 12.

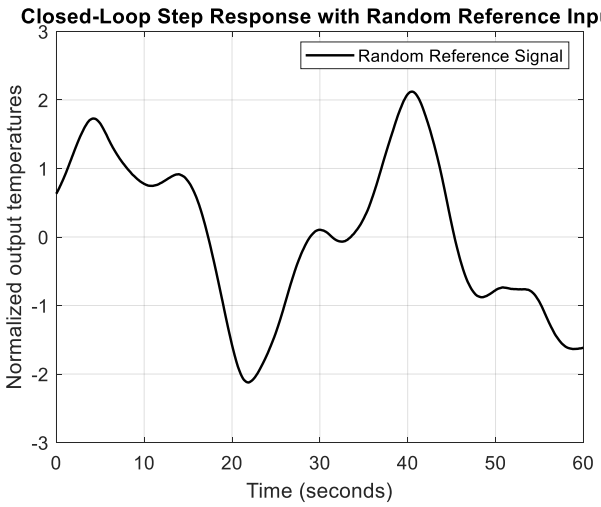

Figure 11. Random reference temperature.

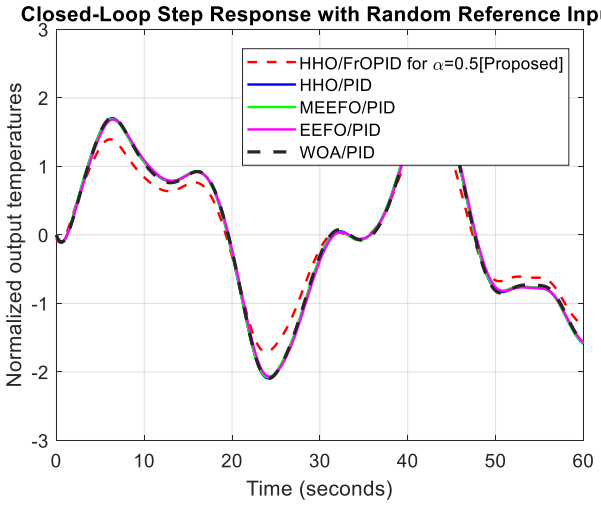

Figure 12. System dynamic response of the fourth scenario.

This figure illustrates the dynamic performance of various controllers, including the proposed HHO/FrOPID controller, in tracking a random reference temperature. The plot highlights each controller's response over time, with the proposed HHO/FrOPID controller exhibiting superior performance in following the random reference signal. The figure clearly demonstrates that the proposed controller outperforms all other controllers."

6. Comparative Analysis with Existing Techniques

This section provides a detailed comparison between the proposed FrOPID controller and other established methods, including Genetic Algorithm (GA) [24], Ziegler-Nichols (ZN) [11], Cohen-Coon (CC) [11], and Direct Synthesis (DS) [11]-based PID controllers. The evaluation considers both time-domain and frequency-domain performance indicators, offering a comprehensive understanding of the relative effectiveness of these techniques.

Figure 13 presents the comparative step responses, allowing for a visual assessment of the dynamic performance of systems controlled by HHO/FrOPID versus the previously discussed methods.

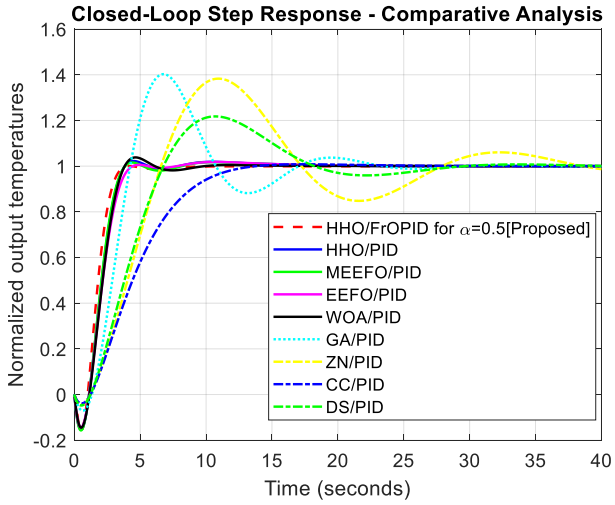

Figure. 13 Comparative step responses with reported methods.

Table 8 presents a comparative analysis of various controllers based on their transient response characteristics. The bolded values indicate the best-obtained performance metrics for each column.

Table 8. Comparative Analysis of the Transient Response

Controllers	T_r [s]	T_s [s]	OS [%]	T_p [s]	**ZLG_Approach1**
HHO/FrOPID [Proposed]	**1.6547**	**3.4335**	**0.1127**	**4.1842**	**1.2615**
HHO/PID	1.8711	5.4817	3.8198	4.6407	2.2885
MoFPA/PID	4.4	20	18	-	-
MoFPA/PIDA	6	20	3.5	-	-
EWOA	6.1	12.5	1	-	-
EWOA + BE	6.3	12.5	0.5	-	-
WOA/PID	2.0340	4.0257	1.8420	10.7431	1.4556
GA/PID	2.1995	21.6536	40.2737	6.7514	10.369
ZN/PID	4.0796	44.9312	38.2960	10.8928	21.041
CC/PID	6.9250	11.7900	0.8071	17.3547	2.8873
DS/PID	4.1622	26.2945	21.7668	10.7035	11.628

Bold refers to the best-obtained value
HHO/FrOPID; Harris hawks optimization based on Fractionalized PID controller, HHO/PID: harris hqwks optimization based PID, MoFPA/PID: modified flower pollination algorithm based PID, MoFPA/PIDA: modified flower pollination algorithm based PID accelerated, **EWOA:** enhanced version of whale optimization algorithm, **EWOA+BE:** enhanced whale optimization algorithm supported by balloon effect, WOA/PID: of whale optimization algorithm based PID, GA/PID: Genetic Algorithm based PID, ZN/PID: Ziegler-Nichols based PID, CC/PID: Cohen-Coon based PID.

Specifically, the proposed HHO/FrOPID [Proposed] controller demonstrates superior transient response in terms of settling time (T_s), rise time (T_r), overshoot (OS), and peak time (T_p) when compared to other controllers. This suggests that the proposed HHO/FrOPID provides the most balanced and efficient performance across the evaluated criteria.

7. Conclusions

In this paper, a modified PID controller, named the Fractionalized Order PID (FrOPID) controller, for temperature control in electric furnaces was proposed. The FrOPID controller incorporates four control terms: proportional, integral, derivative, and fractional integral order. We use the HHO algorithm with the integral absolute error (IAE) performance criterion to tune the four parameters of the FrOPID controller.

The performance of the FrOPID controller is compared with several integer-order PID controllers, which have been tuned using recent optimization approaches, including HHO/PID, MEEFO/PID, EEFO/PID, and WOA/PID. Through comprehensive analysis and comparisons with state-of-the-art optimization algorithms, we evaluate the capabilities of the FrOPID controller and its potential as a high-performance solution for engineering applications.

In time response analysis, the HHO/FrOPID-controlled temperature system demonstrates superior performance, with faster rise and settling times, reduced overshoot, and shorter peak times compared to other algorithms. In frequency response analysis, the proposed controller exhibits robustness and stability, achieving infinite phase margins, high gain margins, and wider bandwidths. The FrOPID controller's superiority is further highlighted through various quality indicators, marking a significant advancement in electric furnace temperature regulation.

As a result of this work, several potential areas for further research have been identified. Investigating the flexibility and effectiveness of the proposed framework in real industrial settings could provide valuable insights into its practical applicability. Additionally, exploring the impact of various environmental conditions and uncertainties on the system could enhance the robustness of the proposed approach. Further research is also needed to examine how the approximation method affects the design of the proposed controller.

Declaration of conflicting interests

The authors affirm no conflicts of interest regarding authorship and research of this article.

Funding

The authors have not received any funding for this research.

References

[1] Li, J. W., Yan, C. F., & Liu, J. (2012). Design of temperature control system based on fuzzy PID. *Advanced Materials Research*, *418*, 1756-1759.

[2] Sheng, T., Luo, H., & Wu, M. (2024). Design and Simulation of a Multi-Channel Biomass Hot Air Furnace with an Intelligent Temperature Control System. *Agriculture*, *14*(3), 419.

[3] Grassi, E., & Tsakalis, K. (2000). PID controller tuning by frequency loop-shaping: application to diffusion furnace temperature control. *IEEE Transactions on Control Systems Technology*, *8*(5), 842-847.

[4] Ajorloo, D., Nazari, M., Nazari, M., Sepehry, N., & Mohammadzadeh, A. (2023). Mathematical modeling and designing an optimized fuzzy temperature controller for a vacuum box electric furnace: Numerical and experimental study. *Transactions of the Institute of Measurement and Control*, *45*(7), 1193-1212.

[5] Pringsakul, N., & Puangdownreong, D. (2020). Mofpa-based pida controller design optimization for electric furnace temperature control system. *Int. J. Innov. Comput. Inf. Control*, *16*(6), 1863-1876.

[6] Liu, L., Xue, D., & Zhang, S. (2023). General type industrial temperature system control based on fuzzy fractional-order PID controller. *Complex & Intelligent Systems*, *9*(3), 2585-2597.

[7] Rsetam, K., Al-Rawi, M., & Cao, Z. (2022). Robust adaptive active disturbance rejection control of an electric furnace using additional continuous sliding mode component. *ISA transactions*, *130*, 152-162.

[8] Goodwin, G. C., Middleton, R. H., Seron, M. M., & Campos, B. (2013). Application of nonlinear model predictive control to an industrial induction heating furnace. *Annual Reviews in Control*, *37*(2), 271-277.

[9] Valarmathi, R., Theerthagiri, P. R., Rakeshkumar, S., & Gomathi, V. (2018, March). Design of genetic algorithm based internal model controller for a heat exchanger. In *2018 International Conference on Computation of Power, Energy, Information and Communication (ICCPEIC)* (pp. 489-495). IEEE.

[10] Jayachitra, A., & Vinodha, R. (2014). Genetic algorithm based PID controller tuning approach for continuous stirred tank reactor. *Advances in Artificial Intelligence*, *2014*(1), 791230.

[11] Sinlapakun, V., & Assawinchaichote, W. (2015, June). Optimized PID controller design for electric furnace temperature systems with Nelder Mead Algorithm. In *2015 12th International Conference on Electrical Engineering/Electronics, Computer, Telecommunications and Information Technology (ECTI-CON)* (pp. 1-4). IEEE.

[12] Jiang, W., & Jiang, X. (2012). Design of an intelligent temperature control system based on the fuzzy self-tuning PID. *Procedia Engineering*, *43*, 307-311.

[13] Zhang, R., Zou, Q., Cao, Z., & Gao, F. (2017). Design of fractional order modeling based extended non-minimal state space MPC for temperature in an industrial electric heating furnace. *Journal of Process Control*, *56*, 13-22.

[14] Liang, H., Sang, Z. K., Wu, Y. Z., Zhang, Y. H., & Zhao, R. (2021). High precision temperature control performance of a PID neural network-controlled heater under complex outdoor conditions. *Applied Thermal Engineering*, *195*, 117234.

[15] Hussein, M. M., Alkhalaf, S., Mohamed, T. H., Osheba, D. S., Ahmed, M., Hemeida, A., & Hassan, A. M. (2022). Modern Temperature Control of Electric Furnace in Industrial Applications Based on Modified Optimization Technique. *Energies*, *15*(22), 8474.

[16] Alzakari, S. A., Izci, D., Ekinci, S., Alhussan, A. A., & Hashim, F. A. (2024). A new control scheme for temperature adjustment of electric furnaces using a novel modified electric eel foraging optimizer. *AIMS Mathematics*, *9*(5), 13410-13438.

[17] Chew, I., Wong, F., Bono, A., Nandong, J., & Wong, K. (2020). Genetic algorithm optimization analysis for temperature control system using cascade control loop model. *International Journal of Computing and Digital Systems*, *9*(1), 119-128.

[18] Phan, V. D., Nguyen, X. H., Dinh, V. N., Dang, T. S., Le, V. C., Ho, S. P., ... & Mai, T. A. (2024). Development of an adaptive fuzzy-neural controller for temperature control in a brick tunnel kiln. *Electronics*, *13*(2), 342.

[19] Idir, A., Bensafia, Y., Khettab, K., & Canale, L. (2023). Performance improvement of aircraft pitch angle control using a new reduced order fractionalized PID controller. *Asian Journal of Control*, *25*(4), 2588-2603.

[20] Idir, A., Bensafia, Y., & Canale, L. (2024). Influence of approximation methods on the design of the novel low-order fractionalized PID controller for aircraft system. *Journal of the Brazilian Society of Mechanical Sciences and Engineering*, *46*(2), 98.

[21] Idir, A., Akroum, H., Tadjer, S. A., & Canale, L. (2023, June). A comparative study of integer order PID, fractionalized order PID and fractional order PID controllers on a class of stable system. In *2023 IEEE International Conference on Environment and Electrical Engineering and 2023 IEEE Industrial and Commercial Power Systems Europe (EEEIC/I&CPS Europe)* (pp. 1-6). IEEE.

[22] Guedida, S., Tabbache, B., Nounou, K., & Idir, A. (2024). Reduced-Order Fractionalized Controller for Disturbance Compensation Based on Direct Torque Control of DSIM With Less Harmonic.

[23] Ousaadi, Z., Akroum, H., & Idir, A. (2024). Robustness Enhancement of Fractionalized Order Proportional Integral Controller for Speed Control of Indirect Field-Oriented Control Induction Motor. *Przeglad Elektrotechniczny*, *2024*(3).

[24] Gani, M.M., Islam, M.S. & Ullah, M.A. (2019). Optimal PID tuning for controlling the temperature of electric furnace by genetic algorithm. *SN Appl. Sci.* **1**, 880.

[25] Bensafia, Y., Khettab, K., & Idir, A. (2022). A novel fractionalized PID controller using the sub-optimal approximation of FOTF. *Algerian Journal of Signals and Systems*, *7*(1), 21-26.

[26] Heidari, A. A., Mirjalili, S., Faris, H., Aljarah, I., Mafarja, M., & Chen, H. (2019). Harris hawks optimization: Algorithm and applications. *Future generation computer systems*, *97*, 849-872.

[27] Y. Bensafia, K. Khettab, and A. Idir, . (2018). An Improved Robust Fractionalized PID Controller for a Class of Fractional-Order Systems with Measurement Noise., International Journal of Intelligent Engineering and Systems, 11(2), 200-207.

[28] Oustaloup, A., Levron, F., Mathieu, B., & Nanot, F. M. (2000). Frequency-band complex noninteger differentiator: characterization and synthesis. *IEEE Transactions on Circuits and Systems I: Fundamental Theory and Applications*, *47*(1), 25-39.

[29] Xue, D., & Chen, Y. (2005, January). Sub-optimum H 2 rational approximations to fractional order linear systems. In *International design engineering technical conferences and computers and information in engineering conference* (Vol. 47438, pp. 1527-1536).

[30] Zhao, W., Wang, L., Zhang, Z., Fan, H., Zhang, J., Mirjalili, S., ... & Cao, Q. (2024). Electric eel foraging optimization: A new bio-inspired optimizer for engineering applications. *Expert Systems with Applications*, *238*, 122200.

[31] Mirjalili, S., & Lewis, A. (2016). The whale optimization algorithm. *Advances in engineering software*, *95*, 51-67.